CrossMark

Increased *in vivo* glial activation in patients with amyotrophic lateral sclerosis: Assessed with [11C]-PBR28

Nicole R. Zürcher[a], Marco L. Loggia[a], Robert Lawson[b], Daniel B. Chonde[a], David Izquierdo-Garcia[a], Julia E. Yasek[b], Oluwaseun Akeju[c], Ciprian Catana[a], Bruce R. Rosen[a], Merit E. Cudkowicz[b], Jacob M. Hooker**,[a], Nazem Atassi*,[b]

[a]A. A. Martinos Center for Biomedical Imaging, Department of Radiology, Massachusetts General Hospital, Harvard Medical School, Charlestown, MA, USA
[b]Neurological Clinical Research Institute (NCRI), Department of Neurology, Massachusetts General Hospital, Harvard Medical School, Boston, MA, USA
[c]Department of Anesthesiology, Massachusetts General Hospital, Harvard Medical School, Boston, MA, USA

ARTICLE INFO

ABSTRACT

Evidence from human *post mortem*, *in vivo* and animal model studies implicates the neuroimmune system and activated microglia in the pathology of amyotrophic lateral sclerosis. The study aim was to further evaluate *in vivo* neuroinflammation in individuals with amyotrophic lateral sclerosis using [11C]-PBR28 positron emission tomography. Ten patients with amyotrophic lateral sclerosis (seven males, three females, 38–68 years) and ten age- and [11C]-PBR28 binding affinity-matched healthy volunteers (six males, four females, 33–65 years) completed a positron emission tomography scan. Standardized uptake values were calculated from 60 to 90 min post-injection and normalized to whole brain mean. Voxel-wise analysis showed increased binding in the motor cortices and corticospinal tracts in patients with amyotrophic lateral sclerosis compared to healthy controls ($p_{FWE} < 0.05$). Region of interest analysis revealed increased [11C]-PBR28 binding in the precentral gyrus in patients (normalized standardized uptake value = 1.15) compared to controls (1.03, $p < 0.05$). In patients those values were positively correlated with upper motor neuron burden scores (r = 0.69, $p < 0.05$), and negatively correlated with the amyotrophic lateral sclerosis functional rating scale (r = −0.66, $p < 0.05$). Increased *in vivo* glial activation in motor cortices, that correlates with phenotype, complements previous histopathological reports. Further studies will determine the role of [11C]-PBR28 as a marker of treatments that target neuroinflammation.

1. Introduction

Amyotrophic lateral sclerosis (ALS) is a neurodegenerative disorder in which upper and lower motor neurons degenerate leading to progressive muscle weakness, respiratory failure and death often within 2–5 years (Ferraiuolo et al., 2011). Riluzole, the only FDA-approved treatment provides a modest survival benefit (Lacomblez et al., 1996),

but there are no available treatments that prevent or stop disease progression and current animal models have not yet successfully predicted treatment response in people (Atassi et al., 2012; Ferraiuolo et al., 2011). A substantial body of evidence implicates the neuroimmune system and specifically activated microglia in ALS pathophysiology (Appel et al., 2011). In *post mortem* studies increased activated microglia are correlated with increased upper motor neuron symptoms and faster disease progression (Brettschneider et al., 2012). Despite years of research, the fundamental question of whether the immune response observed in ALS is primary or secondary, beneficial or harmful, or a combination of both, has not yet been clearly answered.

Given the disconnection between mouse models and human disease, it is critical to develop methods to examine disease biology *in vivo* in patients with ALS. With positron emission tomography (PET) a radiotracer is used to visualize and quantify molecular interactions with high sensitivity. Several PET radiotracers have been developed to image activated microglia and most provide contrast by binding the 18 kDa translocator protein (TSPO), formerly known as the peripheral benzodiazepine receptor (PBR), which is highly

expressed in activated microglia and astrocytes (Brown et al., 2007; Lavisse et al., 2012). The first application of TSPO PET imaging in patients with ALS confirmed widespread microglial activation (Turner et al., 2004). This pioneering study conducted with the radioligand [^{11}C]-(R)-PK11195 showed increased binding in the motor cortex, pons, dorsolateral prefrontal cortex and thalamus in a group of ALS patients. Older generation TSPO radioligands such as [^{11}C]-(R)-PK11195 suffered from high levels of non-specific binding and poor signal-to-background ratio (Kreisl et al., 2010). Increased TSPO expression, assessed using the radioligand [^{18}F]-DPA-714, was subsequently reported in the primary motor cortex, supplementary motor area as well as temporal cortex of patients with ALS, thereby providing additional support for a role for inflammatory processes in ALS (Corcia et al., 2012).

The radioligand [^{11}C]-PBR28, developed at the National Institute of Mental Health, was shown to exhibit 80 times more specific binding compared to [^{11}C]-(R)-PK11195 in rhesus macaques (Kreisl et al., 2010). The aim of this proof-of-concept study was to investigate [^{11}C]-PBR28 binding in a group of individuals with ALS compared to a matched group including for TSPO polymorphism of healthy controls and to investigate whether the [^{11}C]-PBR28 radiotracer could better subcategorize ALS patients based on the anatomical regions with the highest disease burden.

2. Materials and methods

The study was conducted at the Athinoula A. Martinos Center for Biomedical Imaging at Massachusetts General Hospital. The protocol was approved by the Institutional Review Board and the Radioactive Drug Research Committee. All participants provided written informed consent according to the Declaration of Helsinki.

2.1. Participants

Fourteen ALS patients were initially screened for the study. To meet inclusion criteria, participants had to fulfill the revised EL Escorial criteria (Brooks et al., 2000) for possible, probable, probable laboratory-supported or definite ALS, not have any signs of frontotemporal dementia and could not be taking any anti-inflammatory or immunosuppressant medications or benzodiazepines. None of the patients had a familial history of ALS.

[^{11}C]-PBR28, along with all second-generation TSPO radiotracers to date, has differential binding affinity to TSPO depending on an Ala147Thr polymorphism in the TSPO gene with Ala/Ala leading to high-, Ala/Thr to mixed-, and Thr/Thr to low-affinity binding (Kreisl et al., 2013; Owen et al., 2012). This binding affinity difference can be detected by standardized uptake value (SUV) measurements (Yoder et al., 2013), and needs to be controlled for in cross-sectional study designs. All participants were tested for TSPO polymorphism and low affinity binders were excluded, resulting in the exclusion of two individuals with ALS with Thr/Thr Ala147Thr polymorphism. Two additional individuals with ALS were not able to lie comfortably on the scanner table and therefore data could not be acquired.

Of the remaining 10 individuals with ALS who successfully completed scanning, seven had limb-onset ALS and three had bulbar-onset ALS. The clinical outcomes obtained from the participants with ALS included the revised ALS functional rating scale (ALSFRS-R) (Cedarbaum et al., 1999), upper motor neuron burden scale (UMNB) (Ellis et al., 1999), and vital capacity (VC). The ALSFRS-R assesses general functional status and ranges from 48 (normal level of functioning) to 0, with lower scores indicating increased disability. The UMNB measures the following deep tendon (scores 0–4) and pathological reflexes (present − 1 or absent − 0): biceps, brachioradialis, triceps, knee jerk, ankle jerk, Hoffman, Babinski, and jaw jerk. The total UMNB score ranges from 0 to 45,

with 0 representing no reflex involvement, and 45 maximal abnormal UMNB. VC measures respiratory functioning and is expressed as a percentage out of 100%, with 100 being normal and scores below 100 indicating decreased lung capacity. The 10 participants with ALS were compared to 10 healthy controls matched for age and TSPO binding affinity.

2.2. Radiotracer synthesis and data acquisition

[^{11}C]-PBR28 was produced in-house using a procedure modified from the literature (Imaizumi et al., 2007). Briefly, the desmethyl precursor (1.0 mg in 100 μL) was loaded into a 5 mL stainless steel loop for reaction with CH_3I using the Wilson captive solvent method (Wilson et al., 2000). [^{11}C]-PBR28 was purified by reversed-phase chromatography and reformulated by solid-phase extraction in 10% ethanol/saline and then aseptically filtered. The radioligand was injected as slow intravenous bolus, with a median administered dose of 419.49 mBq for patients with ALS and 419.08 mBq for controls. PET data were acquired over 90 min and stored in list-mode format.

Participants were scanned on a Siemens magnetic resonance (MR)/PET scanner consisting of a dedicated brain avalanche photodiode-based PET scanner operating in the bore of a 3 T whole-body MR scanner, and an 8-channel head coil was used. This combined MR/PET scanner allowed the simultaneous acquisition of MR and PET data (Catana et al., 2010). An anatomical scan, a multi-echo MP-RAGE (TR = 2530, TE 1–4 = 1.64, 3.5, 5.36, 7.22 ms, flip angle = 7°, voxel size = 1 mm isotropic) was acquired at the beginning of the scan.

2.3. Data analysis

After acquisition, PET images were reconstructed using the Ordinary Poisson Ordered Subset Expectation Maximization 3D algorithm from prompt coincidences, with corrections for normalization, dead time, isotope decay, photon attenuation and expected random and scatter coincidences. Attenuation correction maps were created using MR-based methods (Izquierdo-Garcia et al., 2014). SUV images were created for radioactivity in the field of view 60–90 min post-radioligand injection. To account for motion that may have occurred between MP-RAGE acquisition and the 60–90 min post-injection time point corresponding to the PET frame of interest, $SUV_{60-90\ min}$ was generated in a two-step procedure. First, a $SUV_{60-90\ min}$ image was created for each subject using an attenuation correction map computed from the native MP-RAGE. Subsequently, a new attenuation map was created based on the registration of the native MP-RAGE with the $SUV_{60-90\ min}$ image obtained in this first reconstruction using FreeSurfer's spmregister. A final $SUV_{60-90\ min}$ was then reconstructed based on this new attenuation correction image well registered with the 60–90 min PET data. Individual $SUV_{60-90\ min}$ images were then registered to MNI (Montreal Neurological Institute) space, spatially smoothed (6 mm full width at half maximum), and intensity-normalized to a mean of 1 ($SUVR_{60-90\ min}$) in order to account for differences in global signal across subjects, as previously done for [^{11}C]-PBR28 (Loggia et al., 2015). $SUVR_{60-90\ min}$ in MNI was then fed into a voxelwise between-group analysis. FSL's randomize was used to perform a permutation-based nonparametric two-sample unpaired t-test (n permutation = 10,000, 5 mm variance smoothing) with TSPO genotype added as a nuisance regressor. Threshold-free cluster enhancement (TFCE) was applied and p values were family-wise error rate (FWE) corrected ($p_{FWE} < 0.05$) (Nichols and Holmes, 2002).

An a priori region of interest for the left and right precentral gyri was selected for each subject using Freesurfer's automated parcellation. Two-tailed Mann–Whitney was used to assess between-group differences. To investigate whether [^{11}C]PBR-28 binding correlated with ALS disease severity, Spearman's r was used to investigate for the presence

of correlation between SUVR$_{60-90\ min}$ of the *a priori* precentral gyrus ROI and UMNB scores, ALSFRS-R, and disease duration.

3. Results

3.1. Study participants

Ten ALS patients (7 males, 3 females, 6 high- and 4 mixed-affinity binders), with a mean age of 53.2 years (SD = 10.8, range 38–68) successfully completed scanning and were compared to healthy controls matched for binding affinity and age (6 males, 4 females, 6 high- and 4 mixed-affinity). Healthy controls were on average 51.1 years old (SD = 11.0, range 33–65). See Table 1.

3.2. Individual data in patients with ALS and group means

Visual inspection of SUVR$_{60-90\ min}$ images revealed regional increase in the precentral gyrus in patients with ALS with limb-onset, and not in the patients with ALS with bulbar-onset disease. See Fig. 1A for individual data projected onto the MNI template and Fig. 1B for means for the ALS group, including comparisons between limb- and bulbar-onset patients, and the control group. Patients with limb-onset weakness showed increased binding in the precentral gyri and patients with bulbar-onset weakness showed increased binding in the brainstem (Fig. 1B, top two rows).

3.3. Whole brain between-group analysis

The unpaired *t*-test conducted on the whole brain static SUVR$_{60-90\ min}$ image showed that the ALS group has increased [^{11}C]-PBR28 binding in the bilateral motor cortices, including the primary motor cortex (M1) and supplementary motor area, as well as in the upper region of the corticospinal tract $p_{FWE} < 0.05$, Fig. 1C. There were no regions in which controls showed increased binding compared to individuals with ALS.

Given that to date only TSPO genotype has been shown to influence [^{11}C]-PBR28 binding, we are reporting the results of a voxelwise analysis, which added only TSPO genotype (Ala/Ala vs. Ala/Thr) as a regressor of no interest. However, an additional analysis conducted using TSPO genotype, as well as age and sex as regressors of no interest, led to the same brain regions being significantly increased in

the ALS vs. control group comparison as the analysis where only TSPO genotype was added as a regressor.

3.4. Region of interest analysis

Compared to controls, individuals with ALS exhibited significantly increased binding in the bilateral precentral gyri, *a priori* identified region of interest. ALS (median, range): 1.15, 1.05–1.30, controls: 1.03, 0.99–1.18, $p < 0.05$ (Fig. 2). In ALS patients, SUVR$_{60-90\ min}$ of the right precentral gyrus was positively correlated with UMNB scores, r = 0.69, $p < 0.05$ (Fig. 3A) and negatively correlated with functional status measured by ALSFRS-R, r = −0.66, $p < 0.05$ (Fig. 3B). Disease duration did not correlate with SUVR$_{60-90\ min}$ in the precentral gyrus.

An exploratory comparison of individuals with limb vs. bulbar onset ALS showed that individuals with limb onset (N = 7) had a significantly higher SUVR$_{60-90\ min}$ than individuals with ALS with bulbar onset (N = 3) in the precentral gyrus ($p < 0.05$).

4. Discussion

Our study demonstrates increased *in vivo* [^{11}C]-PBR28 binding in the motor cortices and corticospinal tract in patients with ALS. This finding is consistent with the first microglial PET study in ALS patients (Turner et al., 2004), as well as histopathological studies reporting increased activated microglia near degenerating motor neurons (Brettschneider et al., 2012; Henkel et al., 2004; Kawamata et al., 1992), suggesting that [^{11}C]-PBR28 PET is a robust candidate as an *in vivo* biomarker of inflammation in ALS. This is the first study conducted in patients with ALS using a second-generation TSPO radioligand, while controlling for TSPO binding affinity genotype. In accordance with our findings, previous studies investigating TSPO binding reported increases in motor cortices (Corcia et al., 2012; Turner et al., 2004). Compared to previous tracers, [^{11}C]-PBR28 SUVR images provide higher contrast in regions of activated glia, which represents a considerable advantage when evaluating neuro-inflammation in individual patients.

Apart from clinical signs, there are no reliable biomarkers of upper motor neuron dysfunction in ALS. [^{11}C]-PBR28 PET could represent a marker of upper motor neuron injury that can complement electromyography as an indicator of lower motor neuron injury. Notably, the individual scores from the UMNB scale and ALSFRS-R were correlated with [^{11}C]-PBR28 binding, suggesting a clinical relevance of brain

Table 1
Participant characteristics.

Subject	TSPO genotype	Age	Sex	Site of onset	Disease duration (months)	VC	ALSFRS-R	UMNB
ALS-1	Ala/Ala	53	M	Left lower limb	26	77	32	39
ALS-2	Ala/Ala	48	M	Left upper limb	22	100	31	25
ALS-3	Ala/Ala	38	F	Left upper limb	9	106	35	35
ALS-4	Ala/Thr	68	M	Right & left lower limbs	21	66	41	21
ALS-5	Ala/Thr	55	M	Right upper limb	16	93	36	28
ALS-6	Ala/Thr	48	M	Right lower limb	11	89	42	34
ALS-7	Ala/Thr	39	M	Right upper limb	57	76	30	33
ALS-8	Ala/Ala	51	M	Bulbar	11	76	45	17
ALS-9	Ala/Ala	66	F	Bulbar	34	78	35	28
ALS-10	Ala/Ala	66	F	Bulbar	13	60	37	25
Mean for ALS	60% Ala/Ala	53.2 ± 10.8	70% M	70% Limb	22.0 ± 14.6	82.1 ± 14.6	36.4 ± 4.9	28.5 ± 6.8
CTRL-1	Ala/Ala	59	M	N/A	N/A	N/A	N/A	N/A
CTRL-2	Ala/Ala	51	M	N/A	N/A	N/A	N/A	N/A
CTRL-3	Ala/Ala	33	M	N/A	N/A	N/A	N/A	N/A
CTRL-4	Ala/Ala	65	F	N/A	N/A	N/A	N/A	N/A
CTRL-5	Ala/Ala	58	F	N/A	N/A	N/A	N/A	N/A
CTRL-6	Ala/Ala	52	F	N/A	N/A	N/A	N/A	N/A
CTRL-7	Ala/Thr	60	M	N/A	N/A	N/A	N/A	N/A
CTRL-8	Ala/Thr	43	M	N/A	N/A	N/A	N/A	N/A
CTRL-9	Ala/Thr	34	M	N/A	N/A	N/A	N/A	N/A
CTRL-10	Ala/Thr	56	F	N/A	N/A	N/A	N/A	N/A
Mean for CTRL	60% Ala/Ala	51.1 ± 11.0	60% M					
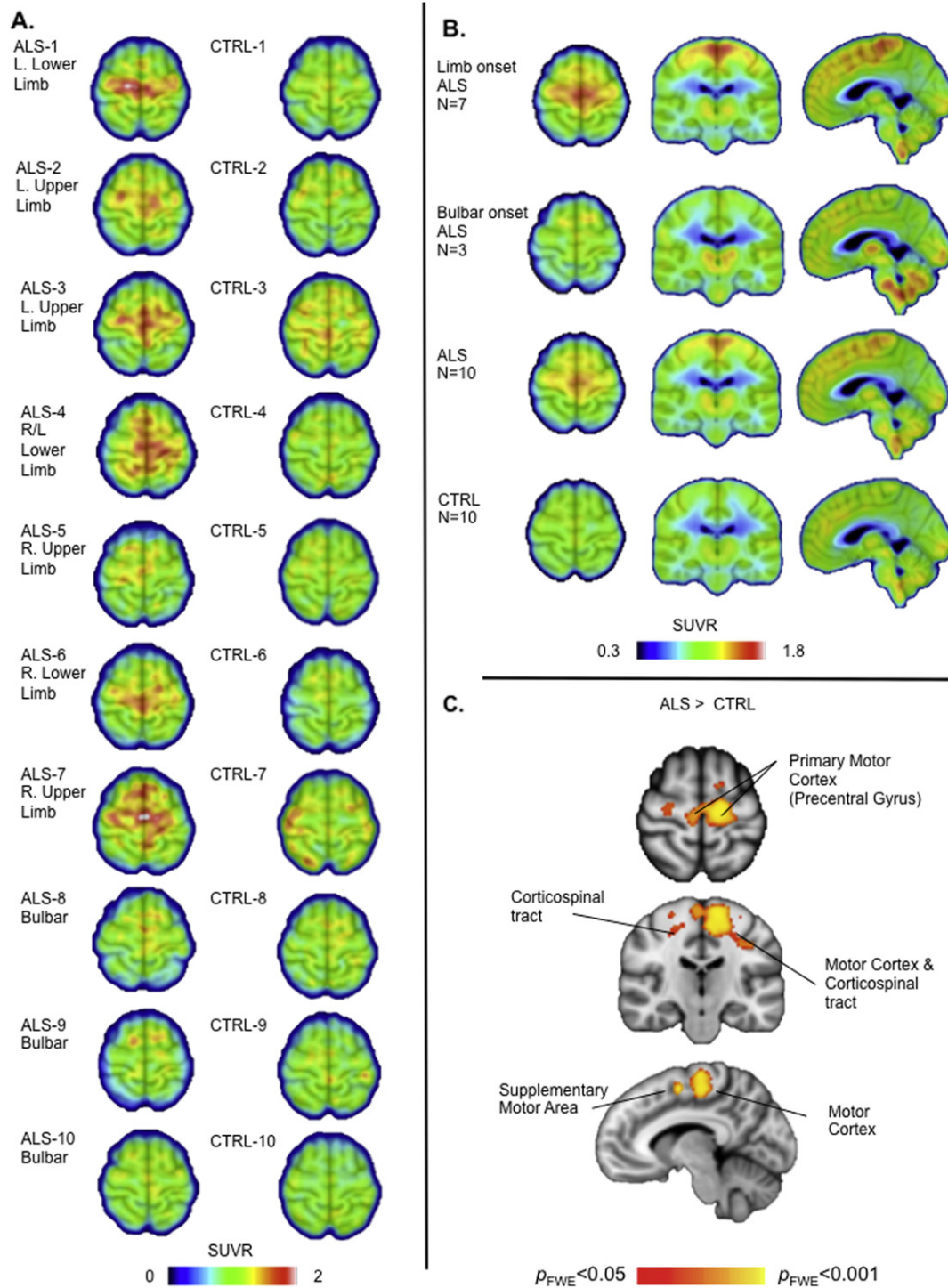
Fig. 1. [^{11}C]-PBR28 SUVR$_{60-90\ min}$ images and statistical maps for between-group differences. A. [^{11}C]-PBR28 SUVR$_{60-90\ min}$ for 10 individual ALS patients and 10 age- and binding affinity-matched healthy controls. SUVR$_{60-90\ min}$ data are projected onto the MNI template in radiological orientation and shown at MNI coordinate z = +64. B. Mean [^{11}C]-PBR28 SUVR$_{60-90\ min}$ images for the ALS and control groups, including comparisons between limb- and bulbar-onset patients, shown at MNI coordinates x = −2, y = −20, and z = +64. C. Brain regions that exhibit significantly higher binding in ALS compared to the control group in the voxelwise whole brain analysis, $p_{FWE} < 0.05$, shown at MNI coordinates x = −8, y = −20, and z = +64.

inflammation measured *in vivo*. Specifically, the UMNB score was positively correlated with microglial PET tracer uptake in the motor cortex using [^{11}C]-PK11195 (Turner et al., 2004). Additionally, our exploratory analysis showed that individuals with bulbar-onset did not show the increased binding in the motor cortex to the extent that it was observed in patients with limb-onset ALS. On the other hand, individuals with bulbar-onset ALS showed regional increases in PBR28 uptake in the

brainstem. This suggests that [^{11}C]-PBR28 binding has a strong anatomical relevance to ALS clinical phenotype (Fig. 1B). The increase in PBR28 uptake in the brainstem could represent inflammation around the lower motor neurons of the cranial nerves as all three bulbar-onset subjects had evidence of lower motor neuron dysfunction on examination. This emphasizes the importance of exploring PBR28 PET imaging in the spinal cord to better characterize this observation. On the other hand,
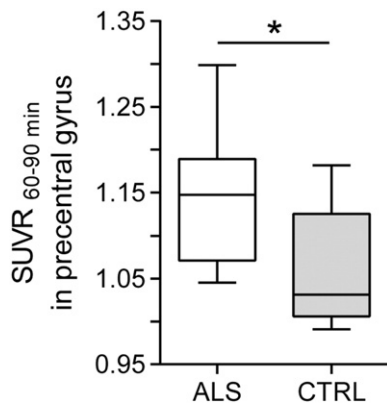
Fig. 2. Increased glial activation in primary motor cortex in ALS. Boxplots for [11C]-PBR28 $SUVR_{60-90 min}$ for the precentral gyrus *a priori* ROI for individuals with ALS and healthy controls. Patients with ALS exhibit significantly increased binding in the motor cortex compared to healthy controls, *$p < 0.05$.

the reason for not seeing increased PBR28 uptake values in the motor cortex in the bulbar-onset patients is unclear. Considering the very small sample size of this subgroup (N = 3) we consider these data preliminary and caution against over-interpretation of these findings.

The main limitation of our study is the relatively small sample size. However, both the two previously published PET studies in ALS using
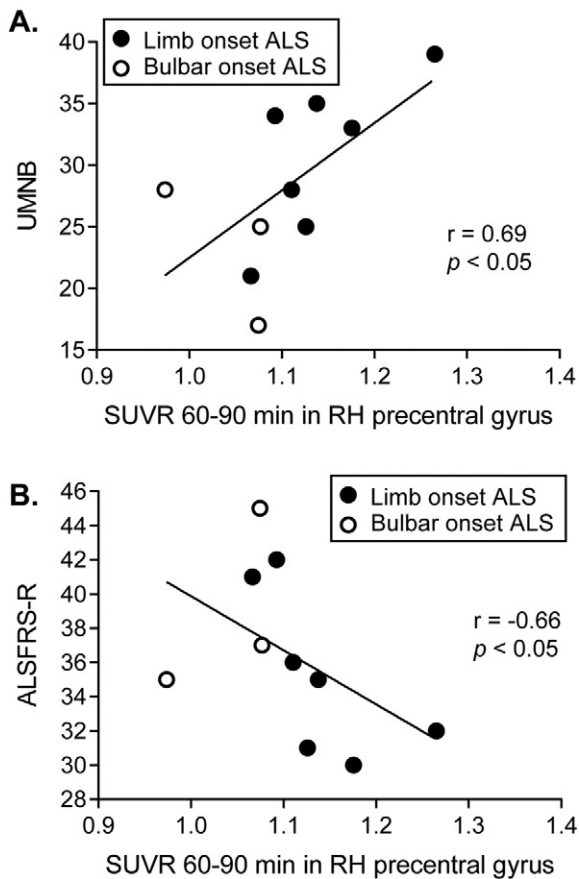

Fig. 3. Correlation between glial activation and ALS disease severity. Significant correlations between [11C]-PBR28 binding in the primary motor cortex and ALS disease severity assessed using UMNB and ALSFRS-R were observed. A. Patients with higher UMNB show increased binding in the motor cortex as shown by a positive correlation between UMNB scores and $SUVR_{60-90 min}$ in the right precentral gyrus *a priori* ROI. B. A negative correlation between the ALSFRS-R and $SUVR_{60-90 min}$ in the right precentral gyrus reflects the fact that patients with a higher disability (lower ALSFRS-R score) show increased PBR28 binding in the motor cortex.

TSPO radiotracers (Corcia et al., 2012; Turner et al., 2004) as well as [11C]PBR28 PET studies in other diseases (Fujita et al., 2013; Oh et al., 2011) have shown that disease-related changes can be observed with comparable sample size. Based on our current findings, larger studies are needed to validate the value of [11C]-PBR28 in ALS and our results should be considered preliminary pending further testing. Forthcoming experiments will help understand how the distribution and degree of [11C]-PBR28 binding change as the disease progresses. Given the preliminary differences observed between individuals with ALS with bulbar onset vs. limb onset ALS, larger studies enrolling more patients with bulbar onset will also be required. In addition, studies enrolling a higher number of participants will help in addressing the topic of laterality. In our study we observed a larger group difference in the left hemisphere and correlation with disease severity only in the right hemisphere. Differences in laterality could be related to handedness of patients, site of onset, or side with most prominent symptoms at time of scan. However, given our sample size, interpretations of laterality are difficult and as previously suggested those questions will need to be addressed in larger studies or meta-analyses (Bede and Hardiman, 2014). Another potential limitation of the current study is the sole use of SUV as representation of [11C]-PBR28 binding without performing kinetic modeling that involves arterial blood sampling. While the potential to use SUV as a binding metric is a promising characteristic for image interpretation, future studies with kinetic modeling derived from arterial blood sampling may need to be conducted to determine binding potential.

The added value of this study lies in the fact that due to the high sensitivity of [11C]-PBR28, increased binding can be observed not only at the group level, but also at the level of individual patients. However, as it currently stands, [11C]-PBR28 PET is not a diagnostic tool for ALS, but rather could serve as a pharmacodynamic biomarker to monitor the efficacy of treatments targeting neuroinflammation. This could be invaluable for evaluation of potential therapeutics in early phase clinical trials. Finally, the current routine ALS trial entry criteria do not include any disease biomarkers and are based solely on phenotype, disability and disease duration. Mechanism-based imaging based on enrollment of individuals with high levels of [11C]-PBR28 binding could help with prognostic stratification or cohort enrichment in ALS clinical trials, as it would allow the selection of ALS patients that have more inflammation at baseline and thus may be more likely to respond to certain treatments. [11C]-PBR28 PET imaging may provide important contributions to the fundamental question of immune system involvement in ALS by allowing a mechanistic investigation of the role of activated microglia. The study of individuals who are pre-symptomatic, but at high risk of developing the disease, such as superoxide dismutase-1 (SOD1) or C9orf72 gene carriers, may also provide important insights in this context, as suggested by a previous PET imaging study investigating pre-symptomatic ALS patients (Turner et al., 2005).

In conclusion, [11C]-PBR28 PET shows increased *in vivo* glial activation in individuals with ALS, supporting a role for glial cells in this disease. Future studies will need to determine its potential as a pharmacodynamic biomarker to monitor the efficacy of treatments targeting neuroinflammation in ALS.

References

Appel, S.H., Zhao, W., Beers, D.R., Henkel, J.S., 2011. The microglial–motoneuron dialogue in ALS. Acta Myol. 30 (1), 4–821842586.

Atassi, N., Schoenfeld, D., Cudkowicz, M., 2012. Clinical trials in amyotrophic lateral sclerosis. In: Ravina, B. (Ed.), Clinical Trials in Neurology. Cambridge University Press, pp. 273–283.

Bede, P., Hardiman, O., 2014. Lessons of ALS imaging: pitfalls and future directions — a critical review. Neuroimage. Clinical 4, 436–443. http://dx.doi.org/10.1016/j.nicl.2014.02.01124624329.

Brettschneider, J., Toledo, J.B., Van Deerlin, V.M., Elman, L., McCluskey, L., Lee, V.M., Trojanowski, J.Q., 2012. Microglial activation correlates with disease progression and upper motor neuron clinical symptoms in amyotrophic lateral sclerosis. PLOS ONE 7 (6), e39216. http://dx.doi.org/10.1371/journal.pone.003921622720079.

Brooks, B.R., Miller, R.G., Swash, M., Munsat, T.L., 2000. El Escorial revisited: revised criteria for the diagnosis of amyotrophic lateral sclerosis. Amyotroph Lateral Scler 1 (5), 293–299. http://dx.doi.org/10.1080/146608200300079536.

Brown, A.K., Fujita, M., Fujimura, Y., Liow, J.-S., Stabin, M., Ryu, Y.H., Imaizumi, M., Hong, J., Pike, V.W., Innis, R.B., 2007. Radiation dosimetry and biodistribution in monkey and man of 11C−PBR28: a PET radioligand to image inflammation. J. Nucl. Med. 48 (12), 2072–2079. http://dx.doi.org/10.2967/jnumed.107.04484218006619.

Catana, C., van der Kouwe, A., Benner, T., Michel, C.J., Hamm, M., Fenchel, M., Fischl, B., Rosen, B., Schmand, M., Sorensen, A.G., 2010. Toward implementing an MRI-based PET attenuation-correction method for neurologic studies on the MR-PET brain prototype. J. Nucl. Med. 51 (9), 1431–1438. http://dx.doi.org/10.2967/jnumed.109.06911220810759.

Cedarbaum, J.M., Stambler, N., Malta, E., Fuller, C., Hilt, D., Thurmond, B., Nakanishi, A., 1999. The ALSFRS-R: a revised ALS functional rating scale that incorporates assessments of respiratory function. BDNF ALS Study Group (Phase III). J. Neurol. Sci. 169 (1–2), 13–21. http://dx.doi.org/10.1016/S0022-510X(99)00210-510540002.

Corcia, P., Tauber, C., Vercoullie, J., Arlicot, N., Prunier, C., Praline, J., Nicolas, G., Venel, Y., Hommet, C., Baulieu, J.L., Cottier, J.P., Roussel, C., Kassiou, M., Guilloteau, D., Ribeiro, M.J., 2012. Molecular imaging of microglial activation in amyotrophic lateral sclerosis. PLOS ONE 7 (12), e52941. http://dx.doi.org/10.1371/journal.pone.005294123300829.

Ellis, C.M., Simmons, A., Jones, D.K., Bland, J., Dawson, J.M., Horsfield, M.A., Williams, S.C., Leigh, P.N., 1999. Diffusion tensor MRI assesses corticospinal tract damage in ALS. Neurol. 53 (5), 1051–1058. http://dx.doi.org/10.1212/WNL.53.5.105110496265.

Ferraiuolo, L., Kirby, J., Grierson, A.J., Sendtner, M., Shaw, P.J., 2011. Molecular pathways of motor neuron injury in amyotrophic lateral sclerosis. Nat. Rev. Neurol. 7 (11), 616–630. http://dx.doi.org/10.1038/nrneurol.2011.15222051914.

Fujita, M., Mahanty, S., Zoghbi, S.S., Ferraris Araneta, M.D., Hong, J., Pike, V.W., Innis, R.B., Nash, T.E., 2013. PET reveals inflammation around calcified Taenia solium granulomas with perilesional edema. PLOS ONE 8 (9), e74052. http://dx.doi.org/10.1371/journal.pone.007405224058514.

Henkel, J.S., Engelhardt, J.I., Siklós, L., Simpson, E.P., Kim, S.H., Pan, T., Goodman, J.C., Siddique, T., Beers, D.R., Appel, S.H., 2004. Presence of dendritic cells, MCP-1, and activated microglia/macrophages in amyotrophic lateral sclerosis spinal cord tissue. Ann. Neurol. 55 (2), 221–235. http://dx.doi.org/10.1002/ana.1080514755726.

Imaizumi, M., Kim, H.J., Zoghbi, S.S., Briard, E., Hong, J., Musachio, J.L., Ruetzler, C., Chuang, D.M., Pike, V.W., Innis, R.B., Fujita, M., 2007. PET imaging with [11C]PBR28 can localize and quantify upregulated peripheral benzodiazepine receptors associated with cerebral ischemia in rat. Neurosci. Lett. 411 (3), 200–205. http://dx.doi.org/10.1016/j.neulet.2006.09.09317127001.

Izquierdo-Garcia, D., Hansen, A.E., Förster, S., Benoit, D., Schachoff, S., Fürst, S., Chen, K.T., Chonde, D.B., Catana, C., 2014. An SPM8-based approach for attenuation correction combining segmentation and nonrigid template formation: application to simultaneous PET/MR brain imaging. J. Nucl. Med. 55 (11), 1825–1830. http://dx.doi.org/10.2967/jnumed.113.13634125278515.

Kawamata, T., Akiyama, H., Yamada, T., McGeer, P.L., 1992. Immunologic reactions in amyotrophic lateral sclerosis brain and spinal cord tissue. Am. J. Pathol. 140 (3), 691–7071347673.

Kreisl, W.C., Fujita, M., Fujimura, Y., Kimura, N., Jenko, K.J., Kannan, P., Hong, J., Morse, C.L., Zoghbi, S.S., Gladding, R.L., Jacobson, S., Oh, U., Pike, V.W., Innis, R.B., 2010. Comparison of [(11)C]-(R)-PK 11195 and [(11)C]PBR28, two radioligands for translocator protein (18 kDa) in human and monkey: implications for positron emission tomographic imaging of this inflammation biomarker. Neuroimage 49, 2924–2932. http://dx.doi.org/10.1016/j.neuroimage.2009.11.05619948230.

Kreisl, W.C., Jenko, K.J., Hines, C.S., Lyoo, C.H., Corona, W., Morse, C.L., Zoghbi, S.S., Hyde, T., Kleinman, J.E., Pike, V.W., McMahon, F.J., Innis, R.B., Biomarkers Consortium PET Radioligand Project Team, 2013. A genetic polymorphism for translocator protein 18 kDa affects both in vitro and in vivo radioligand binding in human brain to this putative biomarker of neuroinflammation. J. Cereb. Blood Flow Metab. 33, 53–58. http://dx.doi.org/10.1038/jcbfm.2012.13122968319.

Lacomblez, L., Bensimon, G., Leigh, P.N., Guillet, P., Meininger, V., 1996. Dose-ranging study of riluzole in amyotrophic lateral sclerosis. Amyotrophic Lateral Sclerosis/Riluzole Study Group II. Lancet 347 (9013), 1425–1431. http://dx.doi.org/10.1016/S0140-6736(96)91680-38676624.

Lavisse, S., Guillermier, M., Hérard, A.-S., Petit, F., Delahaye, M., Van Camp, N., Ben Haim, L., Lebon, V., Remy, P., Dollé, F., Delzescaux, T., Bonvento, G., Hantraye, P., Escartin, C., 2012. Reactive astrocytes overexpress TSPO and are detected by TSPO positron emission tomography imaging. J. Neurosci. 32 (32), 10809–10818. http://dx.doi.org/10.1523/JNEUROSCI.1487-12.201222875916.

Loggia, M.L., Chonde, D.B., Akeju, O., Arabasz, G., Catana, C., Edwards, R.R., Hill, E., Hsu, S., Izquierdo-Garcia, D., Ji, RR., Riley, M., Wasan, A.D., Zürcher, N.R., Albrecht, D.S., Vangel, M.G., Rosen, B.R., Napadow, V., Hooker, J.M., 2015. Evidence of brain glial activation in chronic pain patients. Brain J. Neurol. 138, 604–615. http://dx.doi.org/10.1093/brain/awu377.

Nichols, T.E., Holmes, A.P., 2002. Nonparametric permutation tests for functional neuroimaging: a primer with examples. Hum. Brain Mapp. 15 (1), 1–25. http://dx.doi.org/10.1002/hbm.105811747097.

Oh, U., Fujita, M., Ikonomidou, V.N., Evangelou, I.E., Matsuura, E., Harberts, E., Fujimura, Y., Richert, N.D., Ohayon, J., Pike, V.W., Zhang, Y., Zoghbi, S.S., Innis, R.B., Jacobson, S., 2011. Translocator protein PET imaging for glial activation in multiple sclerosis. J. Neuroimmune Pharmacol. Off. J. Soc. Neuroimmune Pharmacol. 6 (3), 354–361. http://dx.doi.org/10.1007/s11481-010-9243-620872081.

Owen, D.R., Yeo, A.J., Gunn, R.N., Song, K., Wadsworth, G., Lewis, A., Rhodes, C., Pulford, D.J., Bennacef, I., Parker, C.A., StJean, P.L., Cardon, L.R., Mooser, V.E., Matthews, P.M., Rabiner, E.A., Rubio, J.P., 2012. An 18-kDa translocator protein (TSPO) polymorphism explains differences in binding affinity of the PET radioligand PBR28. J Cereb Blood Flow Metab 32 (1), 1–5. http://dx.doi.org/10.1038/jcbfm.2011.147.

Turner, M.R., Cagnin, A., Turkheimer, F.E., Miller, C.C., Shaw, C.E., Brooks, D.J., Leigh, P.N., Banati, R.B., 2004. Evidence of widespread cerebral microglial activation in amyotrophic lateral sclerosis: an [11C](R)-PK11195 positron emission tomography study. Neurobiol. Dis. 15 (3), 601–609. http://dx.doi.org/10.1016/j.nbd.2003.12.01215056468.

Turner, M.R., Hammers, A., Al-Chalabi, A., Shaw, C.E., Andersen, P.M., Brooks, D.J., Leigh, P.N., 2005. Distinct cerebral lesions in sporadic and 'D90A' SOD1 ALS: studies with [11C]flumazenil PET. Brain 128 (6), 1323–1329. http://dx.doi.org/10.1093/brain/awh509.

Wilson, A.A., Garcia, A., Jin, L., Houle, S., 2000. Radiotracer synthesis from [(11)C]-iodomethane: a remarkably simple captive solvent method. Nucl. Med. Biol. 27 (6), 529–532. http://dx.doi.org/10.1016/S0969-8051(00)00132-311056365.

Yoder, K.K., Nho, K., Risacher, S.L., Kim, S., Shen, L., Saykin, A.J., 2013. Influence of TSPO genotype on 11C−PBR28 standardized uptake values. J. Nucl. Med. 54 (8), 1320–1322. http://dx.doi.org/10.2967/jnumed.112.11888523785173.